JACS
JOURNAL OF THE AMERICAN CHEMICAL SOCIETY

Article

pubs.acs.org/JACS

Chemical Environment Control and Enhanced Catalytic Performance of Platinum Nanoparticles Embedded in Nanocrystalline Metal–Organic Frameworks

Kyung Min Choi,[†,§] Kyungsu Na,[†,§] Gabor A. Somorjai,*[,†] and Omar M. Yaghi*[,†,‡]

[†]Department of Chemistry, University of California-Berkeley, Lawrence Berkeley National Laboratory, and Kavli Energy NanoSciences Institute, Berkeley, California 94720, United States

[‡]King Fahd University of Petroleum and Minerals, Dhahran 34464, Saudi Arabia

Supporting Information

ABSTRACT: Chemical environment control of the metal nanoparticles (NPs) embedded in nanocrystalline metal–organic frameworks (nMOFs) is useful in controlling the activity and selectivity of catalytic reactions. In this report, organic linkers with two functional groups, sulfonic acid ($-SO_3H$, S) and ammonium ($-NH_3^+$, N), are chosen as strong and weak acidic functionalities, respectively, and then incorporated into a MOF [$Zr_6O_4(OH)_4(BDC)_6$ (BDC = 1,4-benzenedicarboxylate), termed UiO-66] separately or together in the presence of 2.5 nm Pt NPs to build a series of Pt NPs-embedded in UiO-66 (Pt⊂nUiO-66). We find that these chemical functionalities play a critical role in product selectivity and activity in the gas-phase conversion of methylcyclopentane (MCP) to acyclic isomer, olefins, cyclohexane, and benzene. Pt⊂nUiO-66-S gives the highest selectivity to C_6-cyclic products (62.4% and 28.6% for cyclohexane and benzene, respectively) without acyclic isomers products. Moreover, its catalytic activity was doubled relative to the nonfunctionalized Pt⊂nUiO-66. In contrast, Pt⊂nUiO-66-N decreases selectivity for C_6-cyclic products to <50% while increases the acyclic isomer selectivity to 38.6%. Interestingly, the Pt⊂nUiO-66-SN containing both functional groups gave different product selectivity than their constituents; no cyclohexane was produced, while benzene was the dominant product with olefins and acyclic isomers as minor products. All Pt⊂nUiO-66 catalysts with different functionalities remain intact and maintain their crystal structure, morphology, and chemical functionalities without catalytic deactivation after reactions over 8 h.

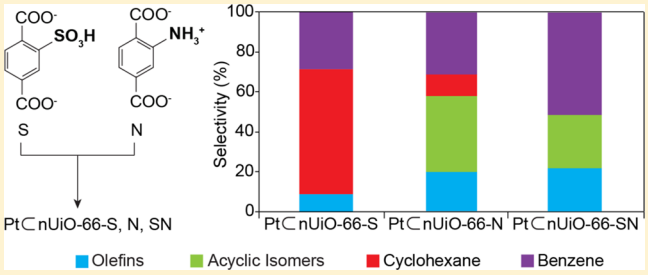

INTRODUCTION

Activity and selectivity in heterogeneous catalysis are highly determined by the structure and chemical properties of the catalyst surface.[1] Typically, methods to enhance the performance of nanocatalysts involve variation of their chemical environment by dispersing them within high surface area supports such as dendrimers, aluminosilicate zeolites, and other porous materials.[2] The catalyst environment in these systems is intrinsically heterogeneous in the spatial arrangement of the chemical functionalities, and therefore it is difficult to control their chemistry and catalytic performance. We recently reported a strategy for embedding Pt nanocatalysts in nanocrystalline metal–organic frameworks (nMOFs) and showed that the ordered structure of the MOF leads to significantly higher activity and selectivity in isomerization reactions of methylcyclopentane (MCP) than Pt nanoparticles (NPs) supported on mesoporous silica used as the reference catalyst.[3] In this report, we take advantage of the facility with which MOFs can be functionalized and show that catalysis by these constructs, Pt⊂nMOFs, is systematically controlled and in some cases enhanced by incorporation of acidic and basic groups, separately or together.

MOFs have been studied with metal NP for their potential application as heterogeneous catalysts. Usually, metal NPs have been introduced by incorporating and reducing metal precursors[4] or by encapsulating them during the synthesis of MOFs[5] for catalysis. This study is an example of how metal catalysts can be precisely designed on their exterior and their environment chemically controlled by using MOFs.

Scheme 1 illustrates the construct of our catalyst and the functionalized nMOFs used in this study. Scheme 1A shows the nMOF without catalyst, the nMOF with Pt NPs on its surface, or incorporated within a single nanocrystal. The earlier two will be used as reference catalysts, and the latter is the construct we studied and for which the chemical functionalities were varied as illustrated in Scheme 1B.

The MOF chosen for this study is $Zr_6O_4(OH)_4(BDC)_6$ (BDC = 1,4-benzenedicarboxylate), termed UiO-66,[6] because its linker, BDC, is easily functionalized with various chemical groups ,and the structure is thermally and chemically stable.[7] In the crystal of UiO-66, each Zr oxide secondary building unit, $Zr_6O_4(OH)_4$(-

Received: April 5, 2015
Published: May 29, 2015

ACS Publications © 2015 American Chemical Society

DOI: 10.1021/jacs.5b03540
J. Am. Chem. Soc. 2015, 137, 7810–7816

Scheme 1. Schematic Representation of All Samples Prepared: (A) Schematic Diagrams for nMOF, Pt-on-nMOF, and Pt⊂nMOF and (B) Combination of Functionalized Linkers Used to Make the nMOFs in the Pt⊂nUiO-66 Constructs

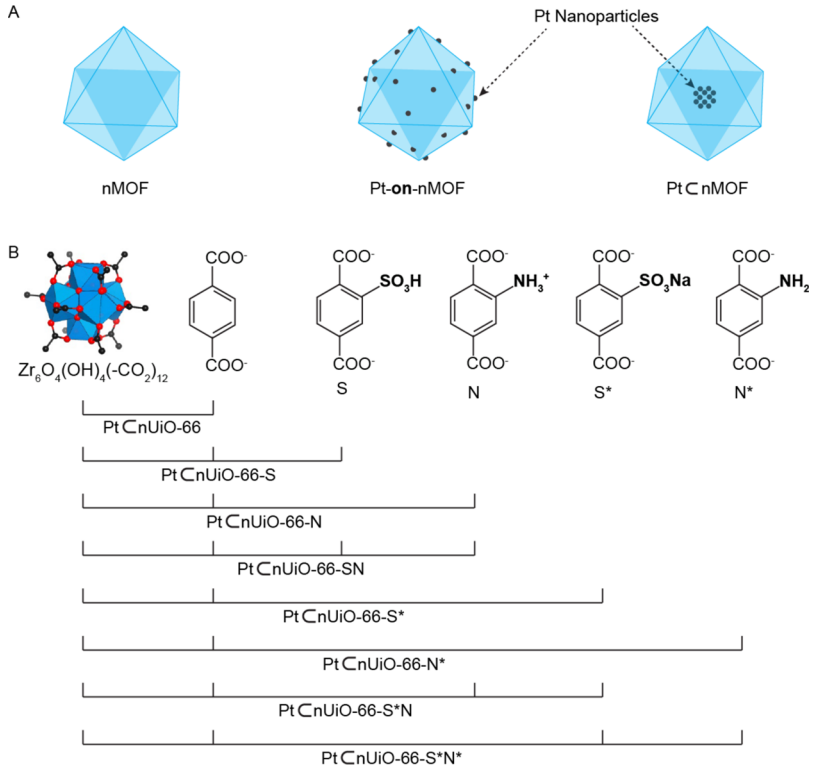

$CO_2)_{12}$, is linked to 12 BDC units to form a porous, three-dimensional framework containing large octahedral (7.2 Å) and small tetrahedral (6.8 Å) pores (Figure 1). Two functional groups of sulfonic acid ($-SO_3H$) and ammonium ($-NH_3^+$) are chosen as chemical functionalities and incorporated separately or together into Pt⊂nUiO-66 (Scheme 1B). The samples functionalized with $-SO_3H$ and $-NH_3^+$ functional groups were named as Pt⊂nUiO-66-S and Pt⊂nUiO-66-N, respectively, and for the sample containing both functional groups was named as Pt⊂nUiO-66-SN (Scheme 1B). As detailed below, the deprotonated forms of $-SO_3H$ and $-NH_3^+$ were obtained by the treatment of these catalysts with NaCl and triethylamine or sodium bicarbonate to give Pt⊂nUiO-66-S*, N*, and S*N* (Scheme 1B).

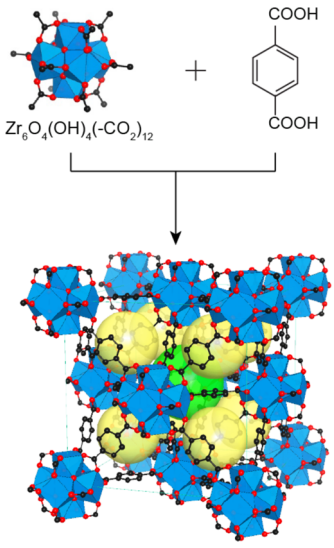

Figure 1. $Zr_6O_4(OH)_4(-CO_2)_{12}$ secondary building units are combined with H_2BDC linkers to form UiO-66, which has a porous, three-dimensional framework containing large octahedral and small tetrahedral cages (filled with green and yellow spheres, respectively). Atom labeling scheme: C, black; O, red; Zr, blue polyhedra. H atoms are omitted for clarity.

EXPERIMENTAL SECTION

Starting Materials. All reagents unless otherwise stated were obtained from commercial sources (Sigma-Aldrich and TCI) and were used without further purification. Specifically, H_2BDC, 2-amino-terephthalic acid (H_2BDC-NH_2), acetic acid, triethylamine (TEA), sodium bicarbonate, *N*,*N*-dimethylformamide (DMF), poly-(vinylpyrrolidone) (PVP), and H_2PtCl_6 were purchased from Sigma-Aldrich. Monosodium salt of 2-sulfonyl terephthalic acid (H_2BDC-SO_3Na) was purchased from TCI.

Characterization of the Catalysts. The crystallinity and porosity of Pt⊂nUiO-66 catalysts and the location and amount of Pt NPs in all samples were characterized by powder X-ray diffraction (PXRD), nitrogen adsorption, transmission electron microscopy (TEM), and inductively coupled plasma atomic emission spectrometry (ICP-AES), respectively. The presence of functional groups in the nMOFs was analyzed by NMR and infrared (IR) spectroscopy. After the catalytic reactions were performed, every sample was analyzed by PXRD, TEM, and NMR to evaluate their structural and chemical stability and detect any organic residues within the catalyst. Hammett acidity was evaluated using an already reported method.[8] Full characterization details are provided in the Supporting Information (SI), Section S1.

Synthesis of Pt Nanoparticles. H_2PtCl_6 (40 mg, 0.098 mmol) was dissolved in 20 mL of ethylene glycol in the presence of 222 mg of poly(vinylpyrrolidone) (PVP, MW = 55,000) in a three-neck round-bottomed flask. This solution was reacted at 180 °C for 10 min, and the as-synthesized PVP-capped Pt NPs were collected by centrifugation, washed, and redispersed in ethanol or DMF to give a colloidal solution of Pt NPs with concentration of 1 mg mL^{-1}. The average size of Pt NPs

DOI: 10.1021/jacs.5b03540
J. Am. Chem. Soc. 2015, 137, 7810−7816

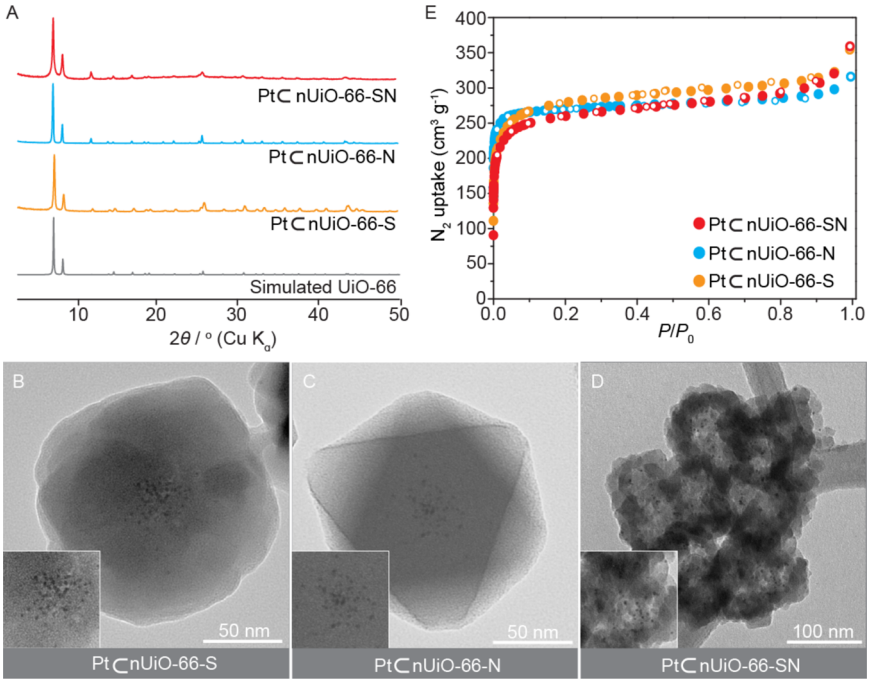

Figure 2. Characterization of PtCnUiO-66-S, N, and SN: (A) PXRD patterns in comparison with simulated pattern of UiO-66, (B–D) TEM image of (B) PtCnUiO-66-S, (C) N, and (D) SN, and (E) N_2 adsorption isotherms at 77 K with adsorption and desorption points represented by closed circles and open circles, respectively (P/P_0, relative pressure).

was 2.5 nm (Figure S1 in SI), and the product from single batch was used for all PtCnUiO-66 catalysts in this study.

Synthesis of PtCnUiO-66-S, N, and SN. $ZrCl_4$ (34.9 mg, 0.15 mmol), acetic acid (0.7 mL), and the acid form of the corresponding organic links [H_2BDC (18.8 mg, 0.113 mmol) and H_2BDC-SO_3Na (10 mg, 0.037 mmol) for PtCnUiO-66-S; H_2BDC (18.8 mg, 0.113 mmol) and H_2BDC-NH_2 (6.8 mg, 0.037 mmol) for PtCnUiO-66-N; H_2BDC (12.5 mg, 0.075 mmol), H_2BDC-SO_3Na (10 mg, 0.037 mmol), and H_2BDC-NH_2 (6.8 mg, 0.037 mmol) for PtCnUiO-66-SN] were mixed in DMF. Then 0.3 mL of Pt NPs in DMF (1 mg mL^{-1}) was added and placed in 120 °C for a day. It is presumed that the acetic acid and HCl (byproduct formed from the hydrolysis of $ZrCl_4$) convert BDC-SO_3Na to BDC-SO_3H and BDC-NH_2 to BDC-NH_3^+ during the reaction (Figure S2 in SI).[9,10] The gray suspensions thus produced were collected and washed three times with DMF using a centrifuge (9000 rpm for 10 min) and sonication and then sequentially immersed in methanol for three 24 h periods. Finally, the samples were activated by removing the solvent under vacuum for 12 h at room temperature. EA of activated sample: Calcd for PtCnUiO-66-S, $Pt_{0.04}Zr_6C_{48}H_{29.02}O_{35.06}S_{1.02}$ = $[Pt_{0.04}Zr_6O_4(OH)_4(BDC\text{-}SO_3H)_{1.02}(BDC)_{4.98}]$: C, 33.00; H, 1.68; S, 0.82%; Found: C, 32.32; H, 3.28; S, 1.30%. Calcd for PtCnUiO-66-N, $Pt_{0.04}Zr_6C_{48}H_{31.06}O_{32}N_{1.02}$ = $[Pt_{0.04}Zr_6O_4(OH)_4(BDC\text{-}NH_3^+)_{1.02}(BDC)_{4.98}]$: C, 34.28; H, 1.87; N, 0.85%; Found: C, 34.23; H, 3.19; N, 3.89%. Calcd for PtCnUiO-66-SN, $Pt_{0.04}Zr_6C_{48}H_{32.98}O_{36.14}S_{1.38}N_{1.20}$ = $[Pt_{0.04}Zr_6O_4(OH)_4(BDC\text{-}SO_3H)_{1.38}(BDC\text{-}NH_3^+)_{1.20}(BDC)_{3.42}]$: C, 32.09; H, 1.85; N, 0.94; S, 1.08%; Found: C, 31.94; H, 3.36; N, 4.14; S, 1.09% Hammett acidity (H_0) of activated sample: PtCnUiO-66-S, −2.4 to −4.4; N, +2.8 to −0.2; SN, −2.4 to −4.4.

Synthesis of PtCnUiO-66-S*, N*, S*N, and S*N*. Each sample of PtCnUiO-66-S, N, and SN was dispersed in 30 mL of water followed by adding sodium chloride (0.1 g) for PtCnUiO-66-S* and S*N and TEA (95 μL) for PtCnUiO-66-N*. In case of PtCnUiO-66-S*N*, sodium bicarbonate (58 mg) was added to the dispersion of PtCnUiO-66-S*N. After 5 min sonication, the resulting samples were washed three times with water using a centrifuge (9000 rpm for 10 min) and then subsequently dried in a freeze drier for 3 days. Hammett acidity (H_0) of activated sample: PtCnUiO-66-S*, N*, and S*N*, no acidity; S*N, +2.8 to −0.2.

Catalytic Reaction Studies. The catalytic testing was performed using a lab-built plug-flow reactor connected to a Hewlett-Packard 5890 gas chromatograph (GC). A 10% SP-2100 on 100/120 Supelco port packed column in line with a flame ionization detector (FID) was used to separate and analyze the C_1–C_6 hydrocarbons. Mass flow controllers were calibrated using a bubble flow meter and used to introduce the ultrahigh purity (99.9999%, Praxair) H_2 and He gases. Saturated vapor pressure of MCP was introduced to the reactor using a bubbler. The reactant flow was carefully calibrated at different temperatures and partial pressures of He carrier. A total flow of 40 mg mL^{-1} was used. Total pressure under flow conditions, measured by using a Baratron capacitance gauge located above the reactor bed, was 790 Torr. Partial pressure of reactants was calculated by using the known temperature vs saturated vapor pressure plots and was 50 Torr with 5:1 H_2 excess. The catalysts (100–150 mg) were diluted by quartz sand with average granular size of 0.4 mm and loaded in the reactor bed. The actual weight of catalyst used was selected to give similar total conversions in each case. The catalysts were reduced at 150 °C for 2 h under a flow of 210 Torr H_2 in 550 Torr He prior to catalytic testing. The catalytic activity and selectivity were evaluated for total conversions below 5%.

RESULTS AND DISCUSSION

Structural and Chemical Analysis of PtCnUiO-66 Catalysts. *Structural Characterization of PtCnUiO-66-S, N, and SN.* The crystallinity of PtCnUiO-66-S, N, and SN was examined by PXRD (Figure 2A), which gave sharp diffraction lines matching those of the simulated pattern obtained from experimental X-ray crystal diffraction data of UiO-66.[6] This clearly indicates preservation of the bulk UiO-66 structure arrangement for nUiO-66 and upon introduction of Pt NPs and the functional groups in PtCnUiO-66-S, N, and SN. TEM images for PtCnUiO-66-S, N, and SN showed Pt NPs embedded inside of nUiO-66 crystals (Figure 2B–D), which is a construct that chemical environment of Pt NPs can be varied using the periodic arrangement of the chemical functionalities in nUiO-66. The permanent porosity of all these samples was preserved as confirmed by measurement of the N_2 adsorption isotherms

DOI: 10.1021/jacs.5b03540
J. Am. Chem. Soc. 2015, 137, 7810–7816

(Figure 2E). They showed Type I isotherms similar to those of bulk UiO-66 and nUiO-66.[6] Langmuir surface areas for PtCnUiO-66-S, N, and SN are 1290, 1200, and 1200 $m^2\ g^{-1}$, respectively; values similar to those found for UiO-66 (1180–2200 $m^2\ g^{-1}$)[3,6] due to the identical structure and porosity. ICP-AES revealed that the amount of Pt for these samples is 0.4 wt %.

Characterization of Functional Groups in PtCnUiO-66-S, N, and SN. The presence of functional groups in PtCnUiO-66-S, N, and SN was first confirmed by IR spectroscopy, where a peak at 1070 cm^{-1} was observed for PtCnUiO-66-S and SN and assigned to the symmetric O=S=O stretch,[10] while a peak at 770 cm^{-1} was observed for PtCnUiO-66-N and SN and assigned to N–H stretch[11] (Figure 3A). This result also indicates that the chemical groups of SO_3H and NH_3^+ remain unchanged during the synthesis.

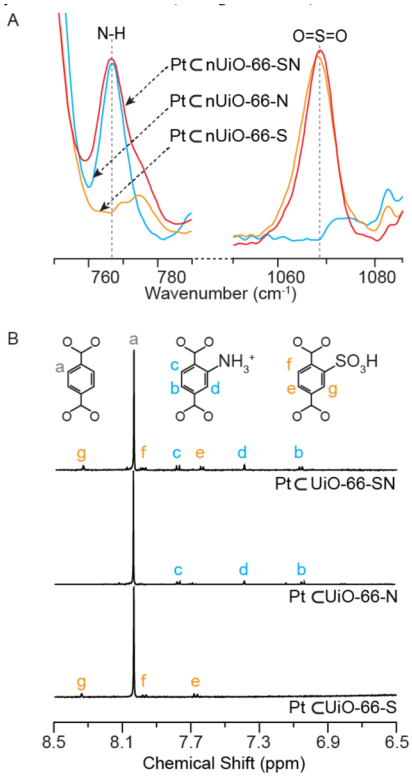

Figure 3. Chemical characterization of PtCnUiO-66-S, N, and SN: (A) IR spectroscopy for the presence of functional groups [*Y*-axis: Absorbance (a.u.)], and (B) ^{1}H NMR spectrum of digested samples for the ratio of functional groups.

The content of functional group for all catalysts was obtained from the ^{1}H NMR spectra of a HF-digested solution of these samples (Figure 3B). The ratios of functional groups were found to be PtCnUiO-66-S, $Zr_6O_4(OH)_4(BDC\text{-}SO_3H)_{1.02}(BDC)_{4.98}$; PtCnUiO-66-N, $Zr_6O_4(OH)_4(BDC\text{-}NH_3^+)_{1.02}(BDC)_{4.98}$; PtCnUiO-66-SN, $Zr_6O_4(OH)_4(BDC\text{-}SO_3H)_{1.38}(BDC\text{-}NH_3^+)_{1.20}(BDC)_{3.42}$. The absence of sodium in PtCnUiO-66-S was confirmed by ICP-AES, where no sodium ions were detected. This indicates that all sodium ions were exchanged with protons during the synthesis and PtCnUiO-66-S contains $-SO_3H$ as previously observed.[9] The $-NH_3^+$ functional group in PtCnUiO-66-N was observed upon addition of TEA. Deprotonation was followed by monitoring the ^{1}H NMR resonance peaks of the methylene protons at 2.4 ppm, which shift to 3.0 ppm as deprotonation proceeds and as triethylammonium is formed (see Figure S2 in SI).

Hammett Acidity of PtCnUiO-66-S, N, and SN. The acidities were evaluated by immersing the dried samples in four different Hammett indicator solutions having different Hammett acidity (H_0); 4-phenylazoaniline (+2.8), 2-nitroaniline (−0.2), 4-nitrodiphenylamine (−2.4), and 2,4-dinitroaniline (−4.4).[8] According to this analysis, PtCnUiO-66-S showed color changes in all indicator solutions except 2,4-dinitroaniline. This indicates that the PtCnUiO-66-S possessed H_0 values between −2.4 and −4.4 (Table 1), which is comparable to *p*-toluenesulfonic acid (H_0 = −2.8).[12] In the case of PtCnUiO-66-N, the color change was observed only in 4-phenylazoaniline, indicating that the PtCnUiO-66-N possessed H_0 values between +2.8 and −0.2 (Table 1), which is comparable to the protonated aniline (H_0 = 4.87).[13] In the case of PtCnUiO-66-SN, this sample showed similar H_0 values (−2.4 to −4.4) to the PtCnUiO-66-S as the acidity of $-SO_3H$ is stronger than that of $-NH_3^+$ (Table 1).

Characterization of PtCnUiO-66-S, N*, S*N, and S*N*.* The crystallinity, porosity, amount, and position of Pt and ratio of functional groups for PtCnUiO-66-S*, N*, S*N, and S*N* did not show a significant change compared to their protonated analogues. (Figures S3–S5 in SI). Their nonacidic nature was confirmed by the lack of color change in the Hammett indicator experiments (Table 1).

Catalytic Conversion of Methylcyclopentane. *PtCnUiO-66-S and N.* Figure 4 shows the catalytic results during the conversion of MCP over PtCnUiO-66-S and N in comparison with Pt-on-SiO_2 and PtCnUiO-66 as the reference catalysts (Scheme 1A). Principally, MCP can be converted to various hydrocarbon species such as (i) olefins, (ii) acyclic isomers, (iii) cyclohexane, (iv) benzene, and (v) cracking products as illustrated in Figure 4A.[3] Pt NPs supported on mesoporous silica (Pt-on-SiO_2) and PtCnUiO-66 were tested as the reference

Table 1. Summary of the Functional Group, Hammett Acidity, and Product Selectivity of PtCnUiO-66 Catalysts

	PtCnUiO-66 catalysts		product selectivity, %			
material	functional group	Hammett acidity H_0	olefin	acyclic isomers	cyclohexane	benzene
Pt-on-SiO_2	N/A	N/A	22.1	**77.9**	N/A	N/A
PtCnUiO-66	N/A	N/A	14.0	22.6	22.2	41.2
PtCnUiO-66-S	$-SO_3H$	−2.4 to −4.4	9.0	N/A	**62.4**	28.6
PtCnUiO-66-N	$-NH_3^+$	+2.8 to −0.2	19.6	38.6	10.6	31.2
PtCnUiO-66-SN	$-SO_3H$ and $-NH_3^+$	−2.4 to −4.4	21.6	26.7	N/A	**51.7**
PtCnUiO-66-S*	$-SO_3Na$	N/A	12.5	27.8	22.6	37.1
PtCnUiO-66-N*	$-NH_2$	N/A	12.8	28.2	23.5	35.5
PtCnUiO-66-S*N	$-SO_3Na$ and $-NH_3^+$	+2.8 to −0.2	18.5	37.6	12.3	31.5
PtCnUiO-66-S*N*	$-SO_3Na$ and $-NH_2$	N/A	18.8	23.7	24.4	33.1

DOI: 10.1021/jacs.5b03540
J. Am. Chem. Soc. 2015, 137, 7810–7816

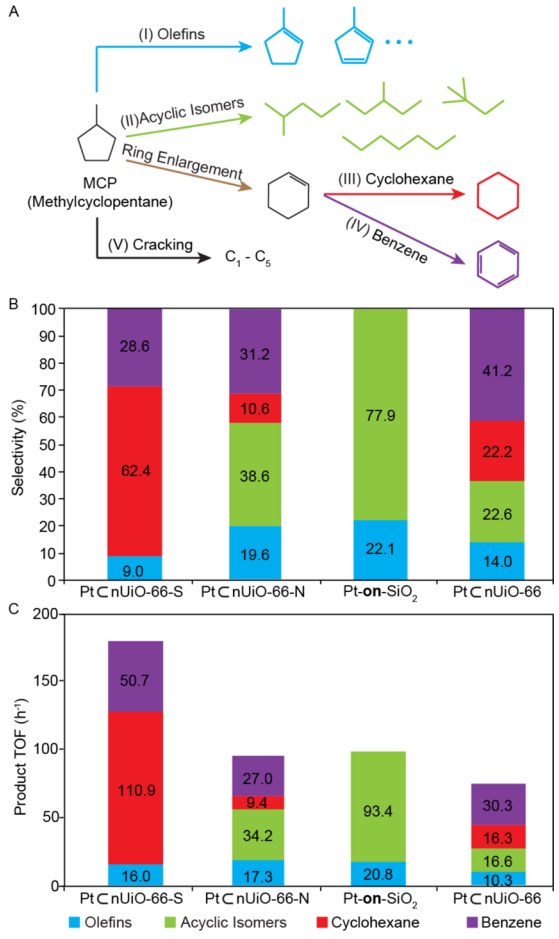

Figure 4. (A) Schematic reaction diagram of conversion of MCP, (B) product selectivity, and (C) turnover frequency (TOF, h^{-1}) obtained at 150 °C over PtCnUiO-66-S and N, PtCnUiO-66, and Pt-on-SiO_2.

catalysts.[3] The Pt-on-SiO_2 reference catalyst produced olefin (22.1%) and acyclic isomers (77.9%) most dominantly, whereas the PtCnUiO-66 gave C_6-cyclic products [cyclohexane (22.2%) and benzene (41.2%)] along with olefin (14.0%) and acyclic isomers (22.6%) (Figure 4B and Table 1). The pure nUiO-66 without Pt NPs showed no activity,[3] which indicates that organic links (BDC), Zr oxide secondary building unit [$Zr_6O_4(OH)_4(-CO_2)_{12}$], and their defective sites[14] do not contribute to the catalytic reaction. However, when $-SO_3H$ or $-NH_3^+$ functional groups were introduced into PtCnUiO-66, the product selectivity was significantly changed. First, PtCnUiO-66-S produced olefin (9.0%), cyclohexane (62.4%), and benzene (28.6%) with no acyclic isomers (Figure 4B and Table 1). To the best of our knowledge, the value (62.4%) for cyclohexane selectivity is the highest reported.[15] In addition, the catalytic activity was enhanced by almost 2-fold as compared to the reference Pt-on-SiO_2 and PtCnUiO-66 (Figure 4C). This would be the synergistic catalytic interplay of Pt NPs and the strong acidic sites originating from the sulfonic acid in the nUiO-66 framework.

The PtCnUiO-66-N having a weak acidic functional group showed different catalytic behavior. It produced less C_6-cyclic products [41.8% including cyclohexane (10.6%) and benzene (31.2%)] than PtCnUiO-66-S [91.0% including cyclohexane (62.4%) and benzene (28.6%)], while the remaining products were acyclic isomers (38.6%) and olefins (19.6%) (Figure 4B,C, and Table 1). The role of weaker acidity appears less significant, as the PtCnUiO-66-N showed lower difference as compared to the PtCnUiO-66. However, due to the presence of acidic sites in PtCnUiO-66-S and N, the activation energy for the formation of benzene and cyclohexane decreased as compared to the catalysts without the acidic functional groups. Among these two catalysts, the PtCnUiO-66-S catalyst showed almost two times higher catalytic activity than PtCnUiO-66-N, which can be explained by the stronger acidity of $-SO_3H$ than that of $-NH_3^+$.

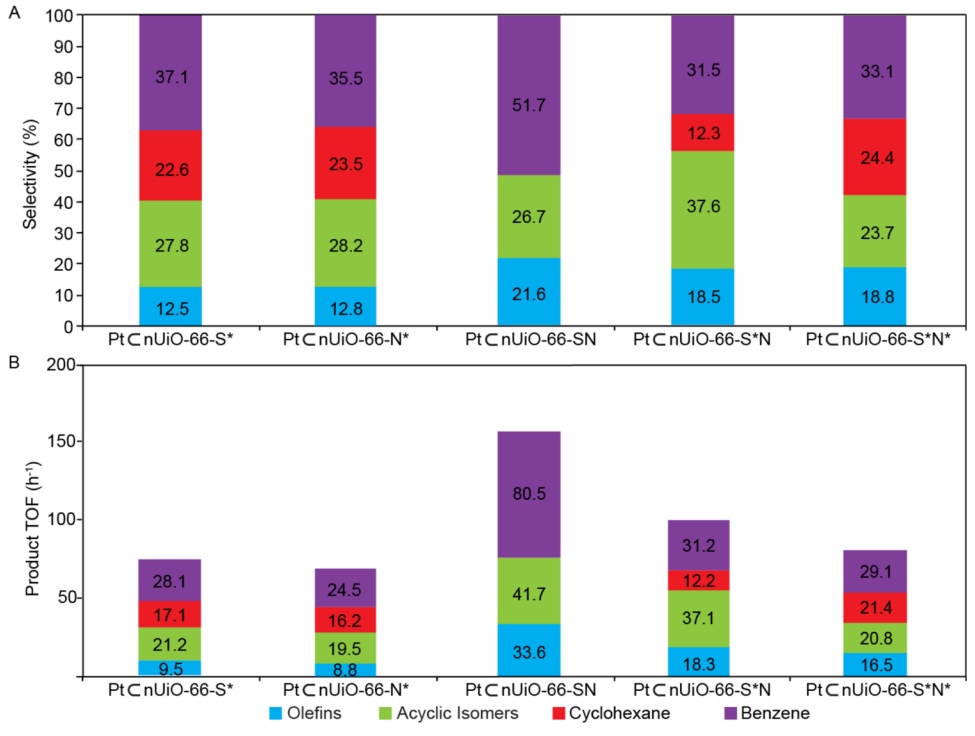

Figure 5. (A) Product selectivity and (B) turnover frequency (TOF, h^{-1}) obtained at 150 °C over PtCnUiO-66-S*, N*, SN, S*N, and S*N*.

DOI: 10.1021/jacs.5b03540
J. Am. Chem. Soc. 2015, 137, 7810−7816

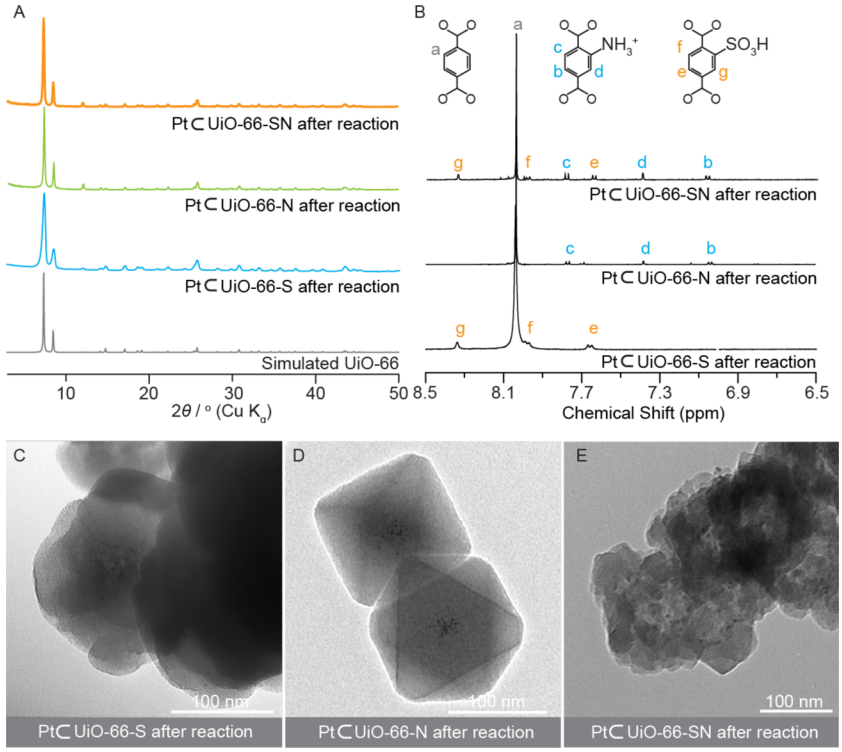

Figure 6. Characterization of Pt⊂nUiO-66-S, N, and SN after catalytic reaction. (A) PXRD patterns of the samples after reaction in comparison with simulated pattern of UiO-66. (B) ^{1}H NMR spectrum of digested samples after reaction and (C–E) TEM images of the samples after reaction.

Pt⊂nUiO-66-S and N**. In order to further study the effect of acidity, the acidic sites in the functional groups of Pt⊂nUiO-66-S and N were neutralized. The catalytic behavior of Pt⊂nUiO-66-S* [olefin (12.5%), acyclic isomers (27.8%), cyclohexane (22.6%), and benzene (37.1%)] and N* [olefin (12.8%), acyclic isomers (28.2%), cyclohexane (23.5%), and benzene (35.5%)] was similar to the reference catalyst (Pt⊂nUiO-66) having no functional groups [olefin (14.0%), acyclic isomers (22.6%), cyclohexane (22.2%), and benzene (41.2%)] (Figure 5A and Table 1), thus indicating the importance of acidity. In addition, their catalytic activity decreased significantly relative to the reference catalyst (Figure 5B). This result implicates that the neutralized functional groups are not making significant catalytic contribution on the change of activity and product selectivity as compared to the nonfunctionalized reference catalyst (i.e., Pt⊂nUiO-66 in Figure 4).

*Pt⊂nUiO-66-SN, S*N, and S*N**. As evidenced above using the Pt⊂nUiO-66-S and N catalysts, the acidic functional groups can control the catalytic reaction. We further introduced the two acidic functional groups with different strengths together into Pt⊂nUiO-66 to make Pt⊂nUiO-66-SN. The Pt⊂nUiO-66-SN changed the product selectivity significantly as shown in Figure 5A and Table 1. Here, no cyclohexane was produced, and the benzene (51.7%) was the dominant product along with olefin (21.6%) and acyclic isomers (26.7%) (Figure 5A and Table 1). It is worth noting that the Pt⊂nUiO-66-S having only $-SO_3H$ functional group gives cyclohexane (62.4%) as the major product with no acyclic isomers (Figure 5A and Table 1). This is an unexpected result where two acidic functional groups with different strengths appear to change the catalytic pathway but keep high activity of the strong acidic functional group (Pt⊂nUiO-66-S); 2-fold increased activity as compared to the reference catalyst and Pt⊂nUiO-66-N (Figure 5B). In this mixed catalyst, we further deprotonated one of two acidic functional groups exclusively or two acidic functional groups simultaneously to make Pt⊂nUiO-66-S*N and S*N*, respectively. The result was that Pt⊂nUiO-66-S*N [olefin (18.5%), acyclic isomers (37.6%), cyclohexane (12.3%), and benzene (31.5%)] behaved like Pt⊂nUiO-66-N and Pt⊂nUiO-66-S*N* [olefin (18.8%), acyclic isomers (23.7%), cyclohexane (24.4%), and benzene (33.1%)] like the reference catalyst (Pt⊂nUiO-66) without functional groups (Figure 5A,B, and Table 1). These results indicate that the protonation of the functional groups is critical for the catalytic performance.

Stability of Pt⊂nUiO-66 Catalysts. The harsh reaction conditions and temperature employed to study these reactions prompted us to examine the recyclability of the chemically functionalized catalysts. Pt⊂nUiO-66-S, N, and SN produced no significant change in catalytic activity and product selectivity while running the catalysts up to three cycles for 8 h (Figure S6 in SI). All tested catalysts were analyzed with PXRD, TEM, and digested NMR to determine their structural and chemical stability (Figure 6). We found that all Pt⊂nUiO-66 catalysts were intact and maintained their crystal structure, morphology and chemical functionalities after the reaction.

■ SUMMARY

We show that the construct of Pt NPs embedded in MOF nanocrystals are ideally suited for altering the chemical environment of the catalyst by virtue of our ability to systematically functionalize the MOF. The principal finding of this study is that the acidic, basic, and neutral functionalities imparted by MOFs with Pt NPs embedded within them do alter the catalytic pathway for MCP conversion, reaction activity, and selectivity. Further, the combination of more than one functionality displays catalytic behavior that is not an intermediary of its constituents, but yields a drastically different ratio of products.

DOI: 10.1021/jacs.5b03540
J. Am. Chem. Soc. 2015, 137, 7810–7816

■ ASSOCIATED CONTENT

Supporting Information

Supplementary characterization of catalysts. The Supporting Information is available free of charge on the ACS Publications website at DOI: 10.1021/jacs.5b03540.

■ AUTHOR INFORMATION

Corresponding Authors

*somorjai@berkeley.edu
*yaghi@berkeley.edu

Author Contributions

§These authors contributed equally.

Notes

The authors declare no competing financial interest.

■ ACKNOWLEDGMENTS

The material synthesis and characterization were supported by BASF SE (Ludwigshafen, Germany) and U.S. Department of Defense, Defense Threat Reduction Agency (HDTRA 1-12-1-0053), respectively, to O.M.Y. G.A.S. acknowledges support by The Chevron Energy Technology Company and from the Director, Office of Science, Office of Basic Energy Sciences, Division of Chemical Sciences, Geological and Biosciences of the U.S. Department of Energy under contract DE-AC02-05CH11231 for catalytic studies. We thank Prof. Peidong Yang for use of the TEM instrument, and Drs. A. M. Fracaroli, P. Siman, and H. Furukawa and Mr. B. Rungtaweevoranit for their valuable discussions and supports.

■ REFERENCES

(1) (a) Balasanthiran, C.; Hoefelmeyer, J. D. Nanocatalysis: Definition and Case Studies. In *Metal Nanoparticles for Catalysis*; Tao, F., Ed.; RSC Catalysis Series No. 17; Royal Society of Chemistry: Cambridge, 2014; pp 6−29. (b) Somorjai, G. A.; Li, Y. *Introduction to Surface Chemistry and Catalysis*, 2nd ed.; Wiley: Hoboken, N.J., 2010.

(2) (a) Crooks, R. M.; Zhao, M.; Sun, L.; Chechik, V.; Yeung, L. K. *Acc. Chem. Res.* **2001**, *34*, 181. (b) Gross, E.; Liu, J. H.-C.; Toste, F. D.; Somorjai, G. A. *Nat. Chem.* **2012**, *4*, 947. (c) Gates, B. C. *Chem. Rev.* **1995**, *95*, 511. (d) Corma, A. *J. Catal.* **2003**, *216*, 298. (e) Taguchi, A.; Schüth, F. *Microporous Mesoporous Mater.* **2005**, *77*, 1. (f) White, R. J.; Luque, R.; Budarin, V. L.; Clark, J. H.; Macquarrie, D. J. *Chem. Soc. Rev.* **2009**, *38*, 481.

(3) Na, K.; Choi, K. M.; Yaghi, O. M.; Somorjai, G. A. *Nano Lett.* **2014**, *14*, 5979.

(4) (a) Jiang, H.-L.; Liu, B.; Akita, T.; Haruta, M.; Sakurai, H.; Xu, Q. *J. Am. Chem. Soc.* **2009**, *131*, 11302. (b) Esken, D.; Turner, S.; Lebedev, O. I.; Van Tendeloo, G.; Fischer, R. A. *Chem. Mater.* **2010**, *22*, 6393. (c) Huang, Y.; Lin, Z.; Cao, R. *Chem.—Eur. J.* **2011**, *17*, 12706. (d) Hermannsdörfer, J.; Friedrich, M.; Miyajima, N.; Albuquerque, R. Q.; Kümmel, S.; Kempe, R. *Angew. Chem., Int. Ed.* **2012**, *51*, 11473. (e) Chen, L.; Chen, H.; Luque, R.; Li, Y. *Chem. Sci.* **2014**, *5*, 3708. (f) Chen, Y.-Z.; Xu, Q.; Yu, S.-H.; Jiang, H.-L. *Small* **2014**, *1*, 71. (g) Guo, Z.; Xiao, C.; Maligal-Ganesh, R. V.; Zhou, L.; Goh, T. W.; Li, X.; Tesfagaber, D.; Thiel, A.; Huang, W. *ACS Catal.* **2014**, *4*, 1340. (h) Li, X.; Guo, Z.; Xiao, C.; Goh, T. W.; Tesfagaber, D.; Huang, W. *ACS Catal.* **2014**, *4*, 3490. (i) Luan, Y.; Qi, Y.; Gao, H.; Zheng, N.; Wang, G. *J. Mater. Chem. A* **2014**, *2*, 20588.

(5) (a) Lu, G.; Li, S.; Guo, Z.; Farha, O. K.; Hauser, B. G.; Qi, X.; Wang, Y.; Wang, X.; Han, S.; Liu, X.; DuChene, J. S.; Zhang, H.; Zhang, Q.; Chen, X.; Ma, J.; Loo, S. C. J.; Wei, W. D.; Yang, Y.; Hupp, J. T.; Huo, F. *Nat. Chem.* **2012**, *4*, 310. (b) Kuo, C.-H.; Tang, Y.; Chou, L.-Y.; Sneed, B. T.; Brodsky, C. N.; Zhao, Z.; Tsung, C.-K. *J. Am. Chem. Soc.* **2012**, *134*, 14345. (c) Ke, F.; Zhu, J.; Qiu, L.-G.; Jiang, X. *Chem. Commun.* **2013**, *49*, 1267. (d) Zhao, M.; Deng, K.; He, L.; Liu, Y.; Li, G.; Zhao, H.; Tang, Z. *J. Am. Chem. Soc.* **2014**, *136*, 1738. (e) Chen, L.; Chen, H.; Li, Y. *Chem. Commun.* **2014**, *50*, 14752. (f) Rösler, C.; Esken, D.; Wiktor, C.; Kobayashi, H.; Yamamoto, T.; Matsumura, S.; Kitagawa, H.; Fischer, R. A. *Eur. J. Inorg. Chem.* **2014**, *32*, 5514. (g) Huang, Y.; Zhang, Y.; Chen, X.; Wu, D.; Yi, Z.; Cao, R. *Chem. Commun.* **2014**, *50*, 10115. (h) Zhang, W.; Lu, G.; Cui, C.; Liu, Y.; Li, S.; Yan, W.; Xing, C.; Chi, Y. R.; Yang, Y.; Huo, F. *Adv. Mater.* **2014**, *26*, 4056. (i) Stephenson, C. J.; Hupp, J. T.; Farha, O. K. *Inorg. Chem. Front.* **2015**, *2*, 448. (j) Ke, F.; Wang, L.; Zhu, J. *Nanoscale* **2015**, *7*, 1201.

(6) (a) Cavka, J. H.; Jakobsen, S.; Olsbye, U.; Guillou, N.; Lamberti, C.; Bordiga, S.; Lillerud, K. P. *J. Am. Chem. Soc.* **2008**, *130*, 13850. (b) Choi, K. M.; Jeong, H. M.; Park, J. H.; Zhang, Y.; Kang, J. K.; Yaghi, O. M. *ACS Nano* **2014**, *8*, 7451.

(7) Kandiah, M.; Nilsen, M. H.; Usseglio, S.; Jakobsen, S.; Olsbye, U.; Tilset, M.; Larabi, C.; Quadrelli, E. A.; Bonino, F.; Lillerus, K. P. *Chem. Mater.* **2010**, *22*, 6632.

(8) (a) Walling, C. *J. Am. Chem. Soc.* **1950**, *72*, 1164. (b) Jiang, J.; Gándara, F.; Zhang, Y.-B.; Na, K.; Yaghi, O. M.; Klemperer, W. G. *J. Am. Chem. Soc.* **2014**, *136*, 12844.

(9) Foo, M. L.; Horike; Satoshi, H.; Fukushima, T.; Hijikata, Y.; Kubota, Y.; Takata, M.; Kitagawa, S. *Dalton Trans.* **2012**, *41*, 13791.

(10) Morris, W.; Doonan, C. J.; Yaghi, O. M. *Inorg. Chem.* **2011**, *50*, 6853.

(11) Jacox, M. E. *J. Phys. Chem. Ref. Data* **2013**, *32*, 1.

(12) Guthrie, J. P. *Can. J. Chem.* **1978**, *56*, 2342.

(13) Hornback, J. M. *Organic Chemistry*; Cengage Learning: Independence, KY, 2005.

(14) Wu, H.; Chua, Y.; Krungleviciute, V.; Tyagi, M.; Chen, P.; Yildirim, T.; Zhou, W. *J. Am. Chem. Soc.* **2013**, *135*, 10525.

(15) (a) Na, K.; Musselwhite, N.; Cai, X.; Alayoglu, S.; Somorjai, G. A. *J. Phys. Chem. B* **2014**, *118*, 8446. (b) Na, K.; Alayoglu, S.; Ye, R.; Somorjai, G. A. *J. Am. Chem. Soc.* **2014**, *136*, 17207.

DOI: 10.1021/jacs.5b03540
J. Am. Chem. Soc. 2015, 137, 7810−7816